Influence of local geometry and transition to dispersive regime by mechanical mixing in porous media

Renaud Duplay[1,2] and Pabitra N. Sen[2]
[1]*École Normale Supérieure, Département de Physique, 24 rue Lhomond, 75005 Paris, France*
[2]*Schlumberger-Doll Research, Old Quarry Road, Ridgefield, Connecticut 06877, USA*
(Received 8 April 2004; revised manuscript received 7 October 2004; published 23 December 2004)

We study dispersion without diffusion via mechanical mixing, starting from the early ballistic regime where the mean-square displacement (MSd) $\langle(\xi-\langle\xi\rangle)^2\rangle \propto t^2$ grows as the elapsed time squared, to the long-time, decoherent, asymptotic regime, where, MSd grows linearly in time. We find in the early time regime, the propagator has a fingerprint of local geometry. The quadratic t^2 term in the MSd may persist if a mechanical parameter $\aleph$, *long-range velocity deviation*, which characterizes the deviation of the long-range mean velocity seen by each particle from the long-range mean velocity of the entire ensemble, is nonzero. The time dependence of dispersion coefficient, even in absence of diffusion, shows a behavior similar to that found in Telegraph equation for diffusion with drift.

DOI: 10.1103/PhysRevE.70.066309 PACS number(s): 47.55.Mh, 05.40.−a

I. INTRODUCTION

The purpose of this paper is to explore aspects of mechanical mixing in hydrodynamic dispersion [1]. Hydrodynamic dispersion, the spreading of molecules by combined effect of convective flow and random diffusion, is an archetype of balance of coherent motion and stochastic diffusion that brings out a host of phenomena, such as an amplification of diffusion coefficient, even in low Reynolds' number, nonchaotic flow.

Taylor showed [1] that in Poiseuille flow in capillary tubes, the mean-square displacement $\langle(\xi-\langle\xi\rangle)^2\rangle$ (where ξ is the displacement of a single particle and $\langle\ldots\rangle$ denotes an ensemble average over all the particles) grows, in the long-time asymptotic regime, linearly in time, $\langle(\xi-\langle\xi\rangle)^2\rangle \propto K_\infty t$. He showed that the hydrodynamic dispersion coefficient, $K_\infty \propto D\mathrm{Pe}^2$, with D being the molecular diffusion coefficient and $\mathrm{Pe}=va/D$ is the Péclet number, with v a characteristic velocity and a the tube radius. In capillaries, the decoherence is provided by diffusion of molecules between different streamlines. In absence of diffusion, the particles on slow stream lines that are near the wall will always lag behind the particles on the faster stream lines and the MSd will grow as $\langle(\xi-\langle\xi\rangle)^2\rangle \propto v^2t^2$. Diffusion allows the slow moving particles to hop onto the faster stream lines and vice versa, and eventually, in the asymptotic limit, the decoherent, linear in time behavior for MSd sets in.

In porous media, there is another source of mixing, viz mechanical mixing [2–6] due to the randomness in flow velocities induced by geometrical randomness. Throughout this paper, we consider only slow, steady, Stoke's flow. The asymptotic behavior of dispersion in porous media is provided by a balance of mechanical mixing and molecular diffusion. Diffusion is purely stochastic, but mechanical mixing with slow flow, which we considered here, arises from the tortuous flow paths that are frozen in time in a stationary regime. Different behaviors for mean-square displacement $\langle(\xi-\langle\xi\rangle)^2\rangle \propto K(t)t$, such as $K(t)/D \propto \mathrm{Pe}$, Pe^2, $\mathrm{Pe}\ln(\mathrm{Pe})$, t^β, $\beta \neq 1$ as a function of Pe, time, etc., have been reported in the literature. These dispersive regimes in porous media have been studied theoretically [2,3,7–9], numerically [10,11] and experimentally [5,6,12–16]. $\mathrm{Pe}\ln(\mathrm{Pe})$ behavior was explained by Saffman [2,3] and later by Baudet *et al.* [8] in specific models.

In this paper we investigate mainly two aspects of mechanical mixing using a simple model: (i) how the local geometry leaves its fingerprint on dispersion and (ii) the manner in which the asymptotic regime sets in.

Regarding the signature of local geometry, we examine how the local features affect the flow propagator, the probability distribution $P(\xi,t)$ of displacements ξ along the direction of macroscopic flow, at time t. One directly measures the Fourier transform of the propagator using Nuclear Magnetic Resonance (NMR) experiments [5,6,12–16]. As pointed out by these authors [6], the NMR propagator experiments give information in micron length scales, a resolution that is not afforded by other imaging techniques, such as MRI, imaging of flow velocities, X-ray tomography, or traditional tracer injection methods. Hulin and his collaborators [6], among others, have emphasized that while much attention has been paid to spreading processes in the field scale dispersion, pore-scale features deserve more attention because they are important in a host of problems in porous media, such as fingering in chromatographic columns [17]. These local features play an important role during transition to asymptotic behavior. In Fig. 4 of Ref. [6] the authors identify correctly the shape of the probability distribution $P(\xi,t)$ for early times with that of the local velocity distribution. More importantly, they draw attention, in their Fig. 6, to a double peaked distribution with a second "bump" that develops for larger displacements, which are comparable to the bead size, and reflects a correlation length L of the Lagrangian velocities of the fluid particles. Clearly, such features in a propagator can be a useful probe of microgeometry.

Our investigation, while greatly influenced by the work of Hulin's group [5,6], is somewhat different in emphasis. First, to study the effect of local geometry, we incorporate local variation in velocities by giving the flow channels a nonuniform cross section. Second, we use only mechanical mixing and develop an explicit formulation for the time-dependent dispersion coefficient $K(t)$.

The second aspect of our study addresses the asymptotic regime where the displacements evolve as a Taylorian-Gaussian that moves with the mean velocity and whose second moment increases linearly in time, $\langle(\xi-\langle\xi\rangle)^2\rangle \propto K_\infty t$. We give a general formulation of dispersion coefficient in terms of a mechanical parameter $\aleph$, *long-range velocity deviation*, that characterizes the deviation of the long-range mean velocity seen by each particle from the long-range mean velocity of the entire ensemble. Parameter $\aleph$ can be used to gauge the importance of diffusion. For example, in a system with dead-end pores, $\aleph \neq 0$ and the asymptotic regime does not set in without the help of stochastic process of diffusion. This is an obvious example where the mean velocities seen by different particles are not the same without diffusion.

There are two nonmechanical dispersion mechanisms mediated by diffusion [18,19]. In the absence of diffusion, particles in a given stream line do not move onto another. In a capillary, without diffusion, there will be no dispersion as each stream line would correspond to a given velocity. This represents a nonmechanical dispersion mechanism, "boundary layer" dispersion that arises due to the nonslip boundary conditions on the solid-fluid interface. The boundary layer dispersion is present in all porous media, even in absence of dead ends, as it arises due to the nonslip boundary condition. This is discussed more precisely by Koch and Brady [18,19]. Likewise, the fluid in a dead-end pore, will have no convective displacement, and the same statistics of displacement for fluid inside and outside dead ends, can be achieved only via diffusion. This is the so called "hold-up" mechanism [18,19]. In porous media the particles that are near a boundary with nearly zero velocity may be able to experience a nonzero velocity, even in the absence of diffusion, when it emerges into an open area. When a path that is mostly fast (away from grains) comes near a path mostly slow (near pore-walls), the effect of diffusion over small distances will be of paramount importance. The boundary effect is healed by diffusion over distances that are much smaller than any other characteristic size.

II. MECHANICAL MODEL FOR DISPERSION WITHOUT DIFFUSION

In this paper we will consider systems without any dead ends. We consider only the effect of velocity variation along a streamline, but assume that all the different streamlines have the same length. The model consists in a bundle of tubes in the spirit of Saffman [2,3]. We differ from Saffman in two important ways: first, we assume that the tubes have nonuniform cross sections (trumpet shape); second, and more importantly, we consider the entire time dependence from the early to late period. Saffman considered only the asymptotic limit, where the use of velocity correlation function (see below) applies. Here each tube is different from the adjoining one—but follows the same statistical laws. Each tube has a random length and a random average cross section. Each trumpet shape crudely mimics the pore space (pore and a throat): the void space in a pack of grains. To simplify the calculations, the trumpets are given exponential shape. We only pay attention to the movement along the axis of the tube x, i.e., one-dimensional movement (transverse motions are neglected), and we assume that the flow is incompressible. Like previous models [2,3,6], the velocity along a streamline has discontinuities at the end of each pore tube, even though we require that the flux of flow (velocity times the cross section) remains continuous throughout.

The propagator of $P(\xi,t)$, the probability density of displacement in time t, is averaged over all initial position according to their density

$$P(\xi,t) \equiv \int_{sample} P(x_0+\xi,x_0,t)\rho(x_0)dx_0. \tag{1}$$

In this equation, $P(x_0+\xi,x_0,t)$ is the probability density of having a displacement equal to ξ in the time t, and $\rho(x_0)$ is the density of particles at the initial position x_0. In this model, $\rho(x_0)\propto a(x_0)$ the local cross section. Because we only consider mechanical mixing, $P(x_0+\xi,x_0,t)=\delta(\xi-\Xi(x_0,t))$, where $\Xi(x_0,t)$ is the function that gives the distance traversed by a particle, starting from x_0 during time t. Incompressibility requires that the population $\rho(x_0)dx_0$ at each slice dx_0 at initial positions x_0 is preserved, such $\rho(x_0)dx_0=\rho(x)dx$, $x=x_0+\Xi(x_0,t)$. In other words, x_0 goes to x after time t and x_0+dx_0 becomes $x+dx$ after the same time, incompressibility implies $\rho(x_0)dx_0=\rho(x)dx$. $\Xi(x_0,t)$ is found for each initial position either by inverting the integral $t=\int_{x_0}^{x_0+\Xi(x_0,t)}dx/v(x)$ or by adding incrementally (deterministic) displacements $d\Xi(x,dt)=v(x)dt$ for a given number n of infinitesimal time steps dt, with $t=ndt$, starting from $\{x_0,t=0\}$. We generate the initial positions of particles using a random number generator adhering to distribution of initial position proportional to $\rho(x_0)$. After each deterministic time step, we update the positions and the local velocities that are preassigned via the shape of the trumpet. Next we present the results of numerical simulations.

First, we assume a plug flow, i.e., the velocity depends only on the projected position on the axis of the motion $v(x,r)=v_0(x)\propto 1/a(x)$. At very short mean displacements, Fig. 1 the distribution of displacements is proportional to the velocity distribution, which, in this case, resembles an exponential profile, as seen in bead pack experiments [5,6]. This is the ballistic regime. When the mean displacement increases, this shape is deformed. The result for $\langle\xi\rangle\sim 0.5\langle L\rangle$ is shown in Fig. 2. Here the characteristic size $\langle L\rangle$ is the mean size of the tubes (pores) in the distribution we have used in our simulation. The shape of $P(\xi,t)$ for small ξ continues to reflect the initial distribution of displacements (i.e., the distribution of velocity in the medium and) a second "bump" develops.

As noted earlier, this second bump has been detected in many NMR experiments of dispersion on bead packs at high Péclet number and for a mean displacement smaller than $\langle L\rangle$ [5,6]. For example, in Ref. [5], $P(\xi,t)$ at $\langle\xi\rangle\sim 0.3\langle L\rangle$ looks exactly like the one we present in Fig. 2. This is the signature of the initial fast particles that have traveled to the next pore [5,6]. When the particles get out of the throat (the narrow part of the opening), they "fall" in a slow part (the wide part of the opening) and accumulate there, which results in this

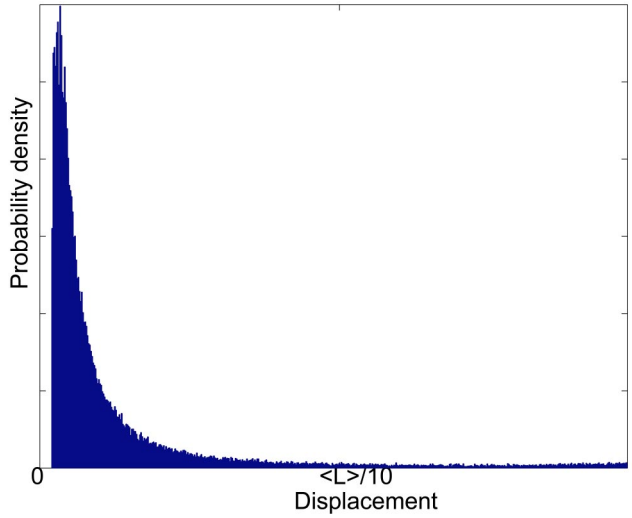

FIG. 1. Distribution of displacements in a plug flow when the mean displacement is small reflects the local velocity distribution.

second bump. This peak is the signature of a "short-range correlation motion" consisting of a sequence of slow-fast-slow, which most of the particle see with a coherent schedule. As the flow is incompressible, there are more particles in the slow part than in the fast part. Thus, the bump is due to the variation of velocity along a streamline (and not due to mixing between the different streamlines themselves).

To check that the variation of velocity along a streamline alone gives the bump, we perform exactly the same simulation as above, but we mimic a Poiseuille flow shape in each tube, $v(x,r)=v_0(x)[1-\pi r^2/a(x)]$, $v_0(x)\propto 1/a(x)$. The propagator simulated at the same mean displacement is shown in Fig. 3. The propagator for Poiseuille flow without diffusion, considered here, is treated as a superposition of one-dimensional flows, one for each streamline corresponding to a given radial position between r_0 and r_0+dr_0. For each streamline, the calculation goes as described above. The radial position of each streamline as it moves down is relocated according to $r_0\rightarrow r'=r_0\sqrt{a(x')/a(x_0)}$, as $x_0\rightarrow x'$. Note

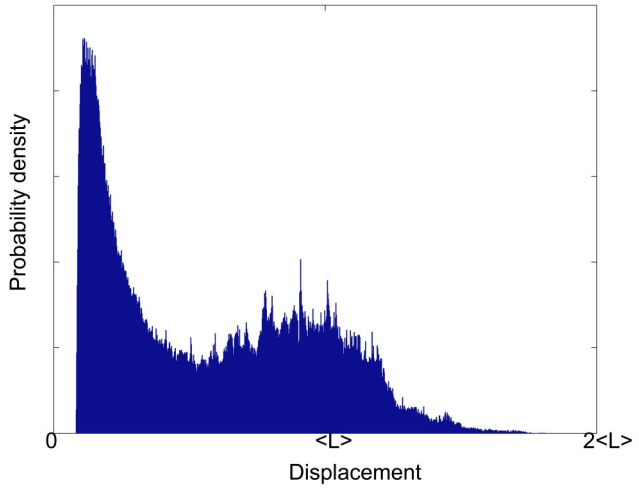

FIG. 2. Distribution of displacements when $\langle\xi\rangle/\langle L\rangle\sim 1/2$ with a plug flow assumption.

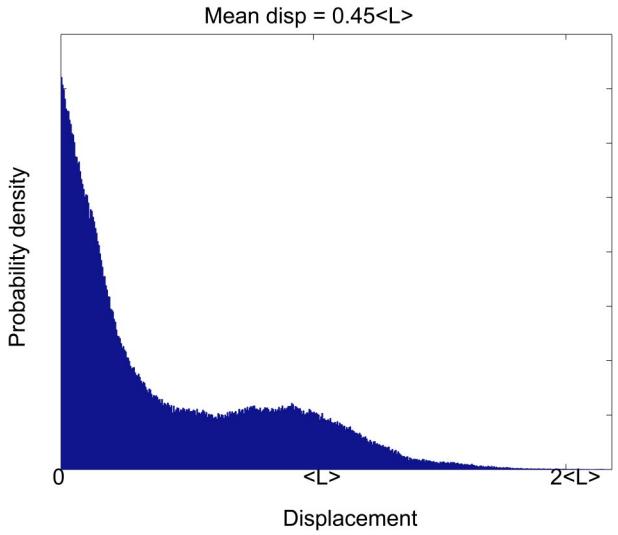

FIG. 3. Distribution of displacements in a Poiseuille flow when the mean displacement is approximatively equal to half the mean size of a pore: $\langle\xi\rangle/\langle L\rangle\sim 1/2$. One can distinctively see a second bump around $\xi=\langle L\rangle$.

that once the distribution of the shapes are chosen, the range of integration for r_0 is defined and factor $[1-\pi r^2/a(x)]$ in $v(x,r)=v_0(x)[1-\pi r^2/a(x)]$ remains invariant down the stream.

Although limited, the Poiseuille flow model considered here is useful in assessing the effects of "slow streamlines" in velocity fluctuations from pore to pore. The model represents an extreme case of the effects of "boundary layer" dispersion [18,19] arising from the nonslip boundary conditions on the solid-fluid interface. The short-range correlation peak is more conspicuous with a plug flow than with a Poiseuille flow. Indeed a Poiseuille flow assumption induces more spread, since the velocity is forced to go to zero, as $r\rightarrow\sqrt{a(x)/\pi}$, at a given position x. Together, these simulations prove that it is really the coherent sequence slow-fast-slow along each streamline plus the incompressible flow assumption that are responsible for the short-range correlation peak. For longer displacement, the second bump will grow further. The peak at the zero displacement peak disappears in the case of the plug flow, but will persist in the case of Poiseuille flow.

Poiseuille flow without diffusion has an anomaly: the zero velocity layers dictated by the boundary condition never disappear and continue to fall back from the remaining group, giving rise to $\langle(\xi-\langle\xi\rangle)^2\rangle\propto t^2$ or $\langle\xi\rangle^2$. In a real system, the transverse molecular diffusion removes the persistence of "zero velocity layer," thus, $\langle(\xi-\langle\xi\rangle)^2\rangle\propto t^2$ or $\langle\xi\rangle^2$ should not be observable in real systems. In other words, the fact that $K(\langle\xi\rangle)$ keeps increasing linearly at long distances in Fig. 4 for the Poiseuille model is due to the lack of transverse diffusion and should not be present in a real system in the asymptotic limit. Next, we turn our attention to this second moment as the descriptor of the mechanical mixing.

The plot in Fig. 4 shows the evolution of $(\langle\xi^2\rangle-\langle\xi\rangle^2)/\langle\xi\rangle$ with $\langle\xi\rangle/\langle L\rangle$. We find that the mean-square displacement $\langle\xi^2\rangle-\langle\xi\rangle^2$ changes from the initial ballistic value

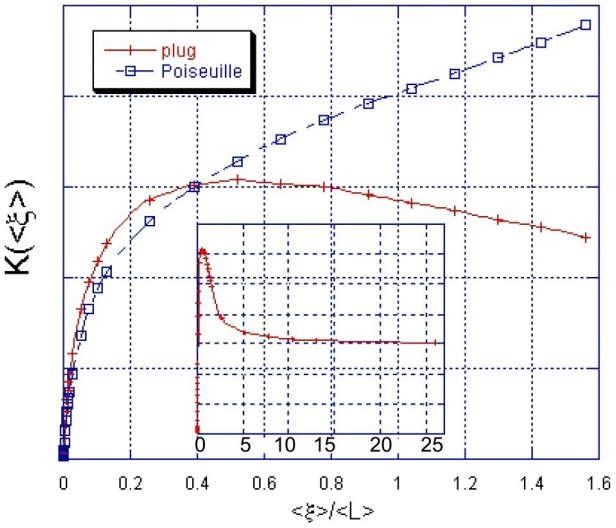

FIG. 4. Mechanical transition of dispersion with Poiseuille flow and plug flow assumptions depicted by the evolution of $K(\langle\xi\rangle \equiv \langle v\rangle t) = (\langle\xi^2\rangle - \langle\xi\rangle^2)/\langle\xi\rangle$. For Poiseuille flow, $K(\langle\xi\rangle)$ changes slope but remains linear in $\langle\xi\rangle$. The inset shows that for the plug flow, $K(\langle\xi\rangle)$ saturates to K_∞ in the asymptotic regime, when $\langle\xi\rangle = \langle v\rangle t \gg \langle L\rangle$.

$(\langle v^2\rangle - \langle v\rangle^2)t^2$ to an asymptotic one, which varies as t^2 or $\langle\xi\rangle^2$ for the Poiseuille flow case, and is linear in t or in $\langle\xi\rangle$ for the plug flow. We are able to fit the transition of the Poiseuille curve quite well by $\exp(-\sqrt{\langle\xi\rangle/l})$ where l is a length around $0.05\langle L\rangle$. By comparing to Fig. 3, one can see that the transition in $\langle\xi^2\rangle - \langle\xi\rangle^2$ occurs while the short-range correlation peak is developing, which allows us to define it as a signature of this mechanical transition. Despite the similarities in the short-range bump in the two propagators for Poiseuille and plug flow, we find in Fig. 4 that the mean-square displacement grows linearly in time or $\langle\xi\rangle$ for plug flow [i.e., $K(t)$] and eventually saturates to its asymptotic value K_∞, in contrast with the Poiseuille flow with no diffusion.

III. VELOCITY-VELOCITY CORRELATION FUNCTION

Next we examine the statistics of the second moment by extending the velocity correlation function formalism. This formalism was originally developed by Taylor [21] and used by Saffman [3], but is often called the Kubo formula. We extend the original formulation by allowing deviations in the mean velocities. We assume that the measurement volume is equal or larger than a representative elementary volume (or REV)—a size on which the medium is homogeneous. In NMR experiments, the signal comes from all the particles enclosed in the pickup coil and we assume that the size of sample seen by the pickup coil is much larger than REV. We suppose that an asymptotic regime exists and that at this time scale, the movement of each particle is decorrelated from the others and follows a time-independent distribution of velocities. Thus, for each particle i, we define the probability law $p_i(v)$, which describes the probability for the particle i to have a velocity between v and $v+dv$. This is equivalent to defining the distribution of velocities that each single particle will encounter along its path across the medium. In the asymptotic regime, $\langle\xi\rangle$ is larger than the characteristic size of a REV. We assume that in the asymptotic limit, the distribution $p_i(v)$ is stable (i.e., has reached a time-independent steady state) for each particle. We now develop $[\langle\xi^2\rangle - \langle\xi\rangle^2](t)$, which we denote by $W(t)$ in this asymptotic regime.

Let $\overline{v_i}$ be the mean with respect to the distribution $p_i(v)$, i.e., the mean of the velocities sampled by the particle i, in its entire course, and, thus, is time independent. The instantaneous velocity is given by a sum of $\overline{v_i}$, and a time-dependent fluctuation term $w_i(t)$: $v_i(t) = \overline{v_i} + w_i(t)$. Then, by assuming that in the asymptotic regime the paths of each particle is uncorrelated from the others, we find

$$W(t) = (\langle\overline{v_i}^2\rangle - \langle\overline{v_i}\rangle^2)t^2 + 2t\int_0^\infty \langle w_i(0)w_i(t)\rangle dt. \qquad (2)$$

As before, $\langle\ldots\rangle$ denotes an average with respect to all the particles (i.e., all tubes and all streamlines). Let us emphasize that the second term in Eq. (2) is a measure of the fluctuations around the mean of each distribution of velocities. It produces a term linear in t in the asymptotic limit, and the integral gives the hydrodynamic dispersion coefficient K_∞. The linear term is the classical expression that goes back, as noted above, to Taylor [21] and to Saffman [3]. Note that these definitions are made from a Lagrangian point of view. Indeed, Saffman [3] termed the velocity-velocity correlation function the Lagrangian correlation function (see also Bear's book [20], Koch and Brady papers [7,18,19]). The first term in (2) defines $\aleph$, the *long-range velocity deviation*, which is an asymptotic mechanical coefficient. Thus, the asymptotic regime of a purely mechanical dispersion can be written

$$[\langle\xi^2\rangle - \langle\xi\rangle^2](t) = \aleph t^2 + Kt, \qquad (3)$$

where $\aleph$ is the long-range velocity deviation, which represents deviations in coherent motions. Our signal is averaged over all initial positions within REV, it is, thus, impossible for us to observe the transient t^4 calculated by Latini and Bernoff [23], which corresponds to motion of a small packet of particles in a capillary; the initial dimension of the packet being much smaller than the radius of the capillary. In our calculations, such features of selected groups of particles at small scales are averaged over.

Equation (3) suggests an ansatz for the complete range of time for dispersion, with or without diffusion, in a general porous medium

$$[\langle\xi^2\rangle - \langle\xi\rangle^2](t) \simeq \mathcal{R}(t)t^2 + \mathcal{F}(t)t. \qquad (4)$$

We call $\mathcal{R}(t)$ the *remanence function of velocity deviation* and $\mathcal{F}(t)$ the *fluctuation function*. In general, $\mathcal{R}(t)$ and $\mathcal{F}(t)$ will rapidly reach their limiting values, which, respectively, are $\aleph$ and K_∞, in a purely mechanical approach. An exception arises when disorder keeps increasing with the size of the sample as in [24].

The initial behavior for $\langle \xi^2 \rangle - \langle \xi \rangle^2$ is given by the ballistic motion $(\langle v^2 \rangle - \langle v \rangle^2)t^2$. This term is expected to decay as the decoherence develops with time, eventually leaving only the asymptotic $K_\infty t$ term in Eq. (3). The early ballistic regime has been emphasized by several authors— starting with Taylor himself [1,4]—and decoherence due to diffusion removes that term. Here we would like to make the distinction that we consider the eventual loss of this ballistic process by decoherence via mechanical mixing in *absence* of diffusion.

For the plug-flow simulation, shown in Fig. 4, we find that the following equations,

$$\mathcal{R}(t) = \left(\langle v^2 \rangle - \langle v \rangle^2 - \beta \frac{\Delta v \Delta L}{\tau_2} \right) \exp\left(- \sqrt{\frac{t}{\tau_1}} \right),$$

$$\mathcal{F}(t) = \beta \Delta v \Delta L \left[1 - \exp\left(- \frac{t}{\tau_2} \right) \right] \tag{5}$$

fit the simulation results well. Here $\tau_2 \simeq 30\tau_1 \simeq 3\langle T \rangle$ ($\langle T \rangle$ is the mean time required to cross a pore), the constant $\beta \sim 0.1$, and the fluctuations $\Delta v \Delta L$, where $\Delta A = \sqrt{\langle A^2 \rangle - \langle A \rangle^2}$, are given by a random walk type estimation. Note that for plug flow $\mathcal{F}(t)$ has short-time t^2 behavior, which is a hallmark of persistence in random walks [21] as seen in the Telegraph equation [9], and a long tail shown in the inset in Fig. 4. For Poiseuille flow in our tandem of trumpets model, the particles that are close to the walls of one trumpet remain close to the walls of all the subsequent trumpets and, thus, always remain slow in absence of diffusion. $\mathcal{R}(t)$ reaches a nonzero constant limit at long times because of the total lack of transverse molecular diffusion. In a complex porous medium, as time goes by, more and more particles close to the wall reach the end of the slow flow lines where they were trapped and move thereafter on faster lines (see below), i.e., $\mathcal{R}(t) \to 0$.

We repeat that the mixing considered in Eq. (5) is by mechanical means alone. For a persistent random walk model, assuming that the velocity-velocity correlation function [a term analogous to the second term in Eq. (2)] decays exponentially in time, with a time constant τ, Taylor [21] found that MSd goes from t^2 to t in the long-time limit as

$$\langle (\xi - \langle \xi \rangle)^2 \rangle = 2\langle v^2 \rangle \{ \tau t - \tau^2 (1 - e^{-t/\tau}) \} \tag{6}$$

Van den Broeck [4] gives a closed-form solution, similar to Eq. (6) for particles that hop between two layers, each moving with different overall velocities. In Eq. (5), $\mathcal{F}(t)$ derives this behavior from encountering random velocities in its flow history. These flow velocities, which are strongly correlated over a pore, and produce the bump in the propagator at early times, eventually become random in moving from pore to pore due to the geometrical randomness, which is intrinsic in a porous medium.

An asymptotic regime is difficult to achieve even in well-connected systems without dead ends. Tessier *et al.* [11] show that a Gaussian limit is not obtained for the range of their data set. Scheven and Sen [16] have measured a nonvanishing third moment to show clearly that at early stages, the distribution is not a Gaussian. Nevertheless, it is common practice to extract an "effective" dispersion coefficient K from the NMR data and plot it against the Péclet number to study how its behaves. Here we find that $K(t)$ has strong dependence on time (or mean displacement) with characteristic times or displacements reflecting the fluctuations in velocity field, and, as such, $K(t)$ does not have a simple dependence on Pe. Diverse behaviors arise out of the different pathways (depending on Pe, geometry, etc.) that lead to the destruction of initial ballistic behavior and destruction of $\mathcal{R}(t)$. Below we consider, qualitatively, how diffusion affects $\mathcal{R}(t)$.

IV. ROLE OF DIFFUSION AND DEPENDENCE OF *K* ON Pe

In a purely mechanical mixing case, $\lim_{t\to\infty} \mathcal{R}(t) = \aleph$. This may or may not be zero in a real system. Diffusion eventually makes $\mathcal{R}(t) \to 0$. With diffusion, $\mathcal{F}(t)$ starts out being zero at $t=0$, then increases to reach asymptotically to K_∞ the *hydrodynamic dispersion coefficient*.

Maier *et al.* [10] find $K_\infty \propto D\mathrm{Pe}$ in random bead packs and $K_\infty \propto D\mathrm{Pe}^2$ in periodic arrays. This example brings out most vividly the role of balance between mechanical mixing and diffusion and how this balance is reflected on dependence of K_∞ on Pe.

In random bead packs, because of tortuosity, a single—deterministic—streamline will encounter a wide range of velocities. Here even a very inefficient diffusion kills the zero-velocity pathology localized at the wall by mixing the streamlines on a scale (of a boundary layer [18,19]) that is much smaller than a pore size. Subsequently, the tortuosity is responsible for homogenizing the different pathways. One thus finds an asymptotic linear regime, due only to mechanical mixing. Then we expect $K_\infty \sim VL$, i.e., $K_\infty/D \sim \mathrm{Pe}$, which implies that K_∞ does *not* depend on diffusion. The role of diffusion is primarily to cut down the time of residence near a wall, which gives rise to the well-known Pe ln(Pe) term [8] of "hold-up" diffusion. However Pe ln(Pe) correction is small in bead packs [10], i.e., they find $K_\infty/D \sim \mathrm{Pe}$.

In contrast, the flow in periodic arrays allows a free motion along the axis of the flow and nearly all the particles collectively participate to create a nonzero value of $\aleph$. To kill the effect of this nonzero $\aleph$, the diffusion length has to be of the order of the scale of a pore to homogenize the pathways. This case is much more like the original case of dispersion through a capillary [1], and, consequently, it is normal to find $K_\infty/D \sim \mathrm{Pe}^2$.

For a pack of beads, which are porous themselves, $\aleph \neq 0$ due to isolation of some of the intrabead channels and not just due to the immobile layers arising from the nonslip boundary condition. Diffusion in and out of a bead is indispensable, and our picture predicts $K_\infty \propto D\mathrm{Pe}^2$, which was observed experimentally [22].

V. CONCLUSION

In conclusion, the dispersion propagator $P(\xi,t)$ in preasymptotic regime has features (bumps) that reflect local geometry of porous media. The mechanical mixing alone, in plug flow ($\aleph \equiv 0$), causes a transition from the ballistic re-

gime to a stochastic one in a way that is strongly dependent on the geometry: the dispersion coefficient $K(t)$ approaches a time-independent asymptotic value K_∞ with characteristic time constants that reflect fluctuations in local velocity or geometry. In absence of dead ends, only the effects due to the nonslip boundary condition will make $\aleph \neq 0$, but diffusion over small distances can heal the dead layers. Combining model simulation and generalizing the velocity correlation function formalism, we develop physically qualitative explanations of the different regimes of dispersion that have been predicted and measured in different geometries. Assuming that the correction arising due to the nonslip boundary condition is small (i.e., Pe ln(Pe) type terms are small, as noted by Maier *et al.* in bead packs [10]), we have two main dependencies for K_∞/D: if $\aleph \to 0$ by diffusion, we expect $K_\infty/D \sim \mathrm{Pe}^2$ or if $\aleph \equiv 0$ by mechanical mixing (tortuosity), we expect, $K_\infty/D \sim \mathrm{Pe}$. Different Pe and time dependencies arise from relative weights of diffusion versus mechanical mixing that kill the $\aleph$ term.

Let us reiterate that all flow considered here is creeping, slow, steady Stokes flow at low Reynolds number. Dispersion induced by turbulence (that was studied by Taylor as early as 1953 [25]) is outside the scope of this paper.

[1] G. I. Taylor, Proc. R. Soc. London, Ser. A **219**, 186 (1953); **223**, 446 (1954); **225**, 473 (1954).
[2] P. Saffman, J. Fluid Mech. **6**, 321(1959).
[3] P. Saffman, J. Fluid Mech. **7**, 194 (1959).
[4] C. Van den Broeck, "Drunks,Drifts, and Dispersion," Dissertation, Vrije Universiteit Brussels, 1988.
[5] L. Lebon, L. Oger, J. Leblond and J. P. Hulin, Phys. Fluids **8**(2), 293 (1996).
[6] L. Lebon, J. Leblond and J. P. Hulin, Phys. Fluids **9**(3), 481 (1997).
[7] D. Koch and J. Brady, J. Fluid Mech. **154**, 399 (1985).
[8] C. Baudet, E. Guyon and Y. Pomeau, J. Phys. (France) Lett. **46**, 991 (1985).
[9] C. Van den Broeck, Physica A **168**, 677, (1990).
[10] R. Maier, D. M. Kroll, R. S. Bernard, S. E. Howington, J. F. Peters and H. T. Davis, Phys. Fluids **12**, 2065 (2000).
[11] J. J. Tessier, K. J. Packer, F-F. Thovert, and P. M. Adler, AIChE J. **43**, 1653 (1997).
[12] B. Manz, P. Alexander, and L. F. Gladden, Phys. Fluids **11**, 259 (1999).
[13] K. Packer and J. J. Tessier, Mol. Phys. **87**, 267 (1996).
[14] A. Ding and D. Candela, Phys. Rev. E **54**, 656 (1996).
[15] J. D. Seymour and P. T. Callaghan, J. Magn. Reson., Ser. A **122**, 90 (1996).
[16] U. M. Scheven and P. N. Sen, Phys. Rev. Lett. **89**, 254501 (2002).
[17] N. Martys, J. Chromatogr., A **707**, 35 (1995).
[18] D. Koch and J. Brady, Chem. Eng. Sci. **142**, 1377 (1987).
[19] D. Koch and J. Brady, J. Fluid Mech. **180**, 387 (1987).
[20] J. Bear, *Dynamics of Fluids in Porous Materials*, (Dover, New York, 1988).
[21] G. I. Taylor, Proc. London Math. Soc. **20**, 181 (1921).
[22] D. Kandhai, D. Hlushkou, A. G. Hoekstra, P. M. A. Sloot, H. Van As, and U. Tallarek, Phys. Rev. Lett. **88**, 234501 (2002).
[23] M. Latini and A. Bernoff, J. Fluid Mech. **441**, 399 (2001).
[24] G. Matheron and G. de Marsily, Water Resour. Res. **16**, 901 (1980).
[25] G. I. Taylor, Proc. R. Soc. London, Ser. A **223**, 446 (1954).